



Geomatic methods applied to the study of the front position changes of Johnsons and Hurd Glaciers, Livingston Island, Antarctica, between 1957 and 2013

Ricardo Rodríguez Cielos¹, Julián Aguirre de Mata², Andrés Díez Galilea², Marina Álvarez Alonso³, Pedro Rodríguez Cielos⁴, and Francisco Navarro Valero⁵

¹Departamento de Señales, Sistemas y Radiocomunicaciones, ETSI de Telecomunicación, Universidad Politécnica de Madrid, Madrid, Spain

²Departamento de Ingeniería Topográfica y Cartografía, ETSI en Topografía, Geodesia y Cartografía, Universidad Politécnica de Madrid, Madrid, Spain

³Departamento de Lenguajes y Sistemas Informáticos e Ingeniería de Software, ETS de Ingenieros Informáticos, Universidad Politécnica de Madrid, Madrid, Spain

⁴Departamento de Matemática Aplicada, ETSI de Telecomunicación, Universidad de Málaga, Málaga, Spain

⁵Departamento de Matemática Aplicada a las Tecnologías de la Información y las Comunicaciones, ETSI de Telecomunicación, Universidad Politécnica de Madrid, Madrid, Spain

Correspondence to: Ricardo Rodríguez Cielos (ricardo.rodriguez@upm.es)

Received: 8 February 2016 – Published in Earth Syst. Sci. Data Discuss.: 10 March 2016

Revised: 31 July 2016 – Accepted: 2 August 2016 – Published: 18 August 2016

Abstract. Various geomatic measurement techniques can be efficiently combined for surveying glacier fronts. Aerial photographs and satellite images can be used to determine the position of the glacier terminus. If the glacier front is easily accessible, the classic surveys using theodolite or total station, GNSS (Global Navigation Satellite System) techniques, laser-scanner or close-range photogrammetry are possible. When the accessibility to the glacier front is difficult or impossible, close-range photogrammetry proves to be useful, inexpensive and fast. In this paper, a methodology combining photogrammetric methods and other techniques is applied to determine the calving front position of Johnsons Glacier. Images taken in 2013 with an inexpensive nonmetric digital camera are georeferenced to a global coordinate system by measuring, using GNSS techniques, support points in accessible areas close to the glacier front, from which control points in inaccessible points on the glacier surface near its calving front are determined with theodolite using the direct intersection method. The front position changes of Johnsons Glacier during the period 1957–2013, as well as those of the land-terminating fronts of Argentina, Las Palmas and Sally Rocks lobes of Hurd glacier, are determined from different geomatic techniques such as surface-based GNSS measurements, aerial photogrammetry and satellite optical imagery. This provides a set of frontal positions useful, e.g., for glacier dynamics modeling and mass balance studies.

Link to the data repository: <https://doi.pangaea.de/10.1594/PANGAEA.845379>.

1 Introduction: study area and background

Hurd and Johnsons glaciers are located in Hurd Peninsula, Livingston Island, the second largest island of the South Shetland Islands (SSI) archipelago (Fig. 1). Johnsons is a tidewater glacier, calving small icebergs into the proglacial bay known as Johnsons Dock, while the fronts of the various tongues of Hurd Glacier (Argentina, Las Palmas and Sally Rocks) are land-terminating. The three unnamed small sea-terminating glacier basins draining to False Bay, to the south-east of Hurd Peninsula (U1, U2, U3 in Fig. 1), which are very steep and heavily crevassed, are not covered in the current study. Johnsons and Hurd glaciers are polythermal, though Johnsons, as compared with Hurd, has a higher proportion of temperate ice (Navarro et al., 2009). Typical velocities near the calving front of Johnsons Glacier are about 50 m yr^{-1} (Rodríguez, 2014), whereas maximum velocities in Hurd Glacier are reached in its central zone, and are typically around 5 m yr^{-1} (Molina, 2014), decreasing towards the terminal zones, which have been suggested to be frozen to bed on the basis of ground-penetrating radar studies, glacier velocities and geomorphological evidences (Navarro et al., 2009; Molina et al., 2007). The annual average temperature at Juan Carlos I Station (12 m a.s.l., in Hurd Peninsula) between 1988 and 2011 was -0.9°C , with average summer (DJF) and winter (JJA) temperatures of 2.4 and -4.4°C , respectively (Osmanoglu et al., 2014). The main glaciological studies in Hurd Peninsula include cartography of volcanic ash layers (Palà et al., 1999; Ximenis, 2001; Molina, 2014), shallow ice coring (Furdàda et al., 1999), numerical modeling of glaciers dynamics (Martín et al., 2004; Otero et al., 2010), analysis of glacier volume changes 1957–2000 (Molina et al., 2007), seismic and ground-penetrating radar surveys (Benjumea et al., 1999, 2001, 2003; Navarro et al., 2005, 2009), modeling of melting (Jonsell et al., 2012), mass-balance observations (Ximenis et al., 1999; Ximenis, 2001; Navarro et al., 2013) and geomorphological and glacier dynamics studies (Ximenis et al., 2000; Molina, 2014). Glaciological studies covering the whole Livingston Island include the analysis of Livingston ice cap front position changes 1956–1996 (Calvet et al., 1999), ground-penetrating radar surveys (Macheret et al., 2009) and estimates of ice discharge to the ocean (Osmanoglu et al., 2014). The latter study also includes ice-cap-wide mass balance estimates and ice velocity fields determined from satellite synthetic aperture radar measurements.

Focusing on the studies dealing with geomatic techniques, Palà et al. (1999) did photogrammetric work in February 1999 focused on the terminal zone of Johnsons Glacier. However, their study only dealt with cartography of ash layers which originated from the eruptions in the neighboring Deception Island (see inset of Fig. 1). They did not determine Johnsons calving front position, since, due to the location of the observation points on the top of Johnsons/Charrúa Peak (340 m a.s.l., see upper right corner of

Fig. 1), only a small fraction of the south-western part of the calving front was visible. Calvet et al. (1999) did an interesting study of the front position changes of the main basins of Livingston Island during the period 1956–1996, based on the Directorate of Overseas Surveys (DOS, 1968a, b) 1 : 200 000 maps (based, in turn, on the 1956–1957 British aerial photographs), a 1962 satellite photograph (declassified intelligence satellite photography, project code “Argon”, 18 May 1962) and LANDSAT (1986, 1988, 1989) and SPOT (1991, 1996) optical images. However, their study did not cover Hurd Peninsula glacier fronts. Calvet et al. (1999) estimated a reduction of the glacier-covered area of Livingston Island by 4.3 % during the period 1956–1996 (from 734 to 703 km^2). More recently, Osmanoglu et al. (2014), using unpublished outlines for 2004 from Jaume Calvet and David García-Sellés, estimated the glacierized area to be 697 km^2 . Molina et al. (2007) analyzed the volume changes 1957–2000 of Hurd Peninsula glaciers comparing digital elevation models (DEMs) for 1957, obtained by photogrammetric restitution from the British Antarctic Survey (BAS) aerial photographs of 1957 and theodolite and GNSS surface-based measurements in 1999–2001. We note, however, that their photogrammetric restitution was done from paper-printed photos (the only available at that time), while our work is based on a digitization from the original films performed later by the BAS. We also note that Molina et al. (2007) used the 1957 photographs, and not those of 1956 as incorrectly stated in their paper (Rodríguez, 2014). Finally, we note that, although the Randolph Glacier Inventory (Pfeffer et al., 2014), based for the Antarctic peripheral glaciers on the inventory by Bliss et al. (2013), provides outlines for Livingston Island glacier basins, those for Hurd Peninsula are outdated. Bliss’ inventory is mainly based on the Antarctic Digital Database (ADD consortium, 2000), digitized from paper maps, aerial photos and LANDSAT, MODIS and ASTER imagery with a range of dates from 1957 to 2005. In the particular case of Hurd Peninsula, at least some of the data clearly correspond to 1957, because Sally Rocks, Las Palmas and Argentina are classified as sea-terminating (in 1957 their fronts were indeed very close to the coastline), while they are clearly land-terminating since several decades ago.

The current study aims to make available to the scientific community the whole set of front positions of Johnsons Glacier, and Argentina, las Palmas and Sally Rocks fronts of Hurd Glacier, between 1957 and 2013. As discussed above, only some front positions for 1957 and 2000 have been published before (Molina et al., 2007; Navarro et al., 2013) while all others were unpublished so far. There are two main reasons for the interest of these front position changes: (1) the surface mass balance of both Hurd and Johnsons glaciers has been monitored since 2001 as part of the World Glacier Monitoring Service database (<http://wgms.ch>), and the correct estimate of the surface mass balance requires one to know the evolution of the glacier outlines; and (2) the mod-

eling of glacier dynamics requires a precise knowledge of the glacier geometry, including the glacier boundaries, and their evolution in case the model applied is time-dependent. The first subject is particularly relevant, since the glaciers in the Antarctic Peninsula region are an exception among the WGMS-monitored glaciers, in the sense that they have experienced sustained positive surface mass balances starting around 2007–2008. The exclusion of the unnamed glacier basins U1, U2, U3 (Fig. 1) from our study is not relevant, since Hurd and Johnsons glaciers are the only Hurd Peninsula glacier basins included in the WGMS database.

2 Data and methods

2.1 Summary of data

The aerial and satellite photographs, and surface-based photogrammetric and GNSS measurements which form the basis of the present study are summarized below (Rodríguez et al., 2015):

- DOCU 1: flight made by the British Antarctic Survey in December 1957. We have selected a total of 5 frames (X26FID0052130, X26FID0052131, X26FID0052132, X26FID0052160 and X26FID0052161) to study Hurd Peninsula glacier fronts.
- DOCU 2: flight made by the United Kingdom Hydrographic Office (UKHO) in January 1990. We have selected a total of 3 frames (0097, 0098 and 0099) for our study.
- DOCU 3: photogrammetric survey, using metric camera, performed by Palà et al. (1999) from the top of Johnsons Peak in 1999.
- DOCU 4: satellite image obtained by the Quickbird system in January 2010 for Hurd Peninsula.
- DOCU 5: satellite image obtained by the Quickbird system in February 2007 for Hurd Peninsula.
- DOCU 6: inventory of data (2000–2012) by the Group of Numerical Simulation in Science and Engineering (GNSCI, in its Spanish acronym) of Universidad Politécnica de Madrid (several authors are affiliated to this group). These observations are made with GNSS techniques and theodolite and are focused on Sally Rocks, Las Palmas and Argentina land-terminating fronts, excluding the calving front of Johnsons Glacier.
- DOCU 7: photogrammetric survey (using non-metric camera) of the calving front of Johnsons Glacier conducted in February 2013.

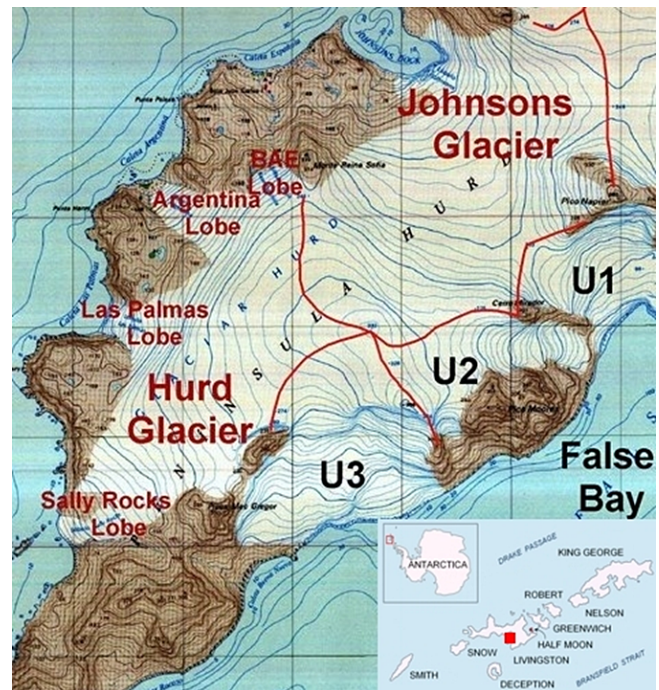


Figure 1. Location of Johnsons and Hurd glaciers in Hurd Peninsula. Base map: 1 : 25 000 map from Geographic Service of the Army (Spain), 1991. The inset shows the location of the South Shetland Islands, and Livingston Island in particular. The red rectangle in the inset indicates the location of Hurd Peninsula.

2.2 Photogrammetry: fundamentals

Photogrammetry is a well-known technique allowing one to obtain three-dimensional information from photographs using stereoscopic vision provided by two different points of view (Wolf, 1983). Its fundamental principle is triangulation. By taking photographs from at least two different locations, so-called “lines of sight” can be traced from each camera to points on the object. These lines of sight (sometimes called rays due to their optical nature) are mathematically intersected to produce the three-dimensional coordinates of the points of interest. This requires a precise knowledge of the position and orientation of the cameras. Resection is the procedure used to determine the position and orientation (also called aiming direction) of the camera, using ground control points appearing on the images that have known coordinates. For a good resection, at least more than 10 well-distributed points in each photograph are needed (Kraus, 1993). Each camera’s position is defined by three coordinates, while three angles are needed to define its orientation. The theoretical central projection can be deformed by lens and film distortion. These influences can be accounted for in a bundle block adjustment by introducing correction polynomials in the observation equations, whose coefficients are determined in the adjustment (Kraus, 2007). The distortion varies with the distance from each point to the center of the optical axis. Dis-

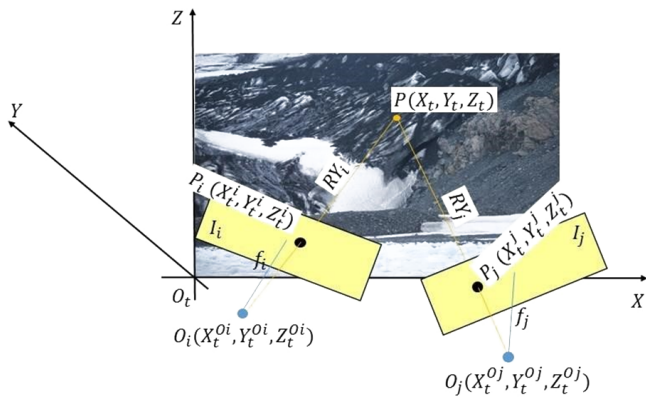


Figure 2. Photogrammetric restitution. By applying spatial similarity transformations (Kraus, 2007), one can calculate the unknown coordinates (X_t, Y_t, Z_t) of a point P from its coordinates P_i and P_j on flat photographs taken from two different points of view O_i and O_j (locations of each camera) with known coordinates.

tortion is often decomposed into radial and tangential components (Brown, 1971), of which the radial is much larger and the tangential is customarily ignored in practice. The radial distortion Δr for a point with image coordinates (x, y) can be expressed as

$$\Delta r = k_1 r^3 + k_2 r^5 + k_3 r^7$$

$$r = \sqrt{(x - x_0)^2 + (y - y_0)^2} \quad (1)$$

where k_i are the coefficients of radial distortion and (x_0, y_0) are the coordinates of the principal point of symmetry (PPS) in the image plane. Once these corrections have been applied, the photogrammetric part of the solution consists of obtaining three-dimensional information from a pair of two-dimensional photographs providing stereoscopic vision. The procedure is illustrated in Fig. 2.

2.3 Photogrammetry of Johnsons Glacier calving front using non-metric camera

We took (February 2013) the photographs of Johnsons Glacier calving front using a non-metric DSLR (Digital Single-Lens Reflex) camera Nikon D60. This is a typical, inexpensive 10 MP digital camera without excessive loss of accuracy. Obviously, its use for photogrammetric purposes requires a photogrammetric calibration, aimed to determine with sufficient accuracy the internal geometry (internal orientation) of the camera. This calibration process involves the use of Eq. (1), to calculate the k_i coefficients and the calibrated focal length. We detail below the main steps of the whole process.

a. Photogrammetric survey

The fieldwork took place in February 2013, under local conditions of few clouds and high visibility (more than 500 m). Several control points were established making

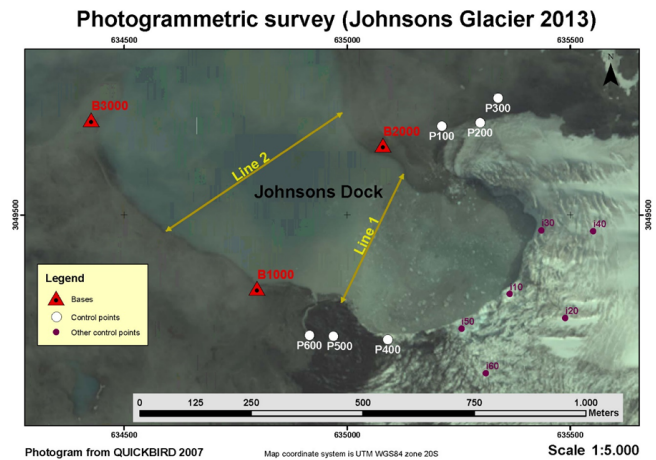


Figure 3. Location of the various kinds of control points. Red triangles: location of the bases, measured using GNSS techniques, where theodolite was positioned (B1000, B2000, B3000). White circles: control points measured using GNSS techniques (P100, P200, P300, P400, P500, P600). Magenta points: other control points, measured using direct intersection method (I10, I20, I30, I40, I50, I60 points). Line 1 and Line 2 represent the zodiac boat tracks from which the photographs were taken. The scale of the figure does not match with the numerical map scale indicated. The latter corresponds to the full-size printed version of the figure. This comment also applies to Figs. 8–12.

a network with permanent base stations near Johnsons Glacier front (Fig. 3, B1000, B2000 and B3000). These bases were measured using GNSS techniques, in particular, a Trimble 5700 GPS with horizontal and vertical accuracies of $\sigma_{xy} = 0.005$ m, $\sigma_z = 0.008$ m respectively. In addition, six control points were measured by the same technique at the sides of the calving front, on lateral moraines (points P100, P200, P300, P400, P500 and P600 in Fig. 3), with accuracies $\sigma_{xy} = 0.011$ m, $\sigma_z = 0.015$ m. These points were marked with red flags, to make them easy to recognize on the photographs. Finally, using a Wild Heerbrugg T1 theodolite, placed at B1000, B2000 and B3000, we measured the coordinates of the control points I10, I20, I30, I40, I50, I60 (Fig. 3) on the terminal part of the glacier (inaccessible because of high crevassing), with accuracies $\sigma_{xz} = 0.17$ m, $\sigma_z = 0.30$ m. We used the direct intersection method by resection from the three bases, allowing for some redundancy in the observations (Domínguez, 1993). T1 theodolite does not allow the measurement of distances, so only angles were measured.

b. Photograph shooting

As mentioned, the camera used is a Nikon D60 DSLR 10 MP camera, with lens 55–200 mm AF-S DX. In our case, the only possibility for taking pictures approximately perpendicular to the glacier calving front (normal photogrammetry) is using a boat. We used a zodiac

boat, taking photos from lines 1 and 2 in Fig. 3. Line 1 is at approximately 400 m distance from the glacier front, and we used a focal length of 95 mm and set the focus to infinity. We used the same focal length and focus to infinity for the photos taken from Line 2, located at an approximate distance of 700 m from the glacier front. The overlap was higher than 95 %. To increase the number of control points over the glacier, we took more pictures from a location near P500. These photographs were taken with a focal length of 130 mm and focus to infinity. In this case we mounted the camera on a tripod over the ground, and took the photos using convergent photogrammetry. We thus obtained coordinates for additional control points (about 20 new points). In these photographs we could also observe three stakes from the net of velocity and mass balance measurements, which are customarily measured using GNSS techniques (Navarro et al., 2013).

c. Camera calibration

Calibration is made both before and after the photographic fieldwork, using the same settings. We chose a building named “Mirador” for calibration, which is located at Princesa de Eboli street in Madrid, which has an ideal configuration for this project (Fig. 4). This building has a large open space (square) at its front, allowing shot distances similar to those used during fieldwork at Johnsons Glacier (400 m). This distance also makes it easy to measure the corners of the windows to be used as calibration grid, using a total station (theodolite plus laser distance meter). For establishing the corners of the reticle, windows situated in a lower horizontal line, an upper horizontal line, two central horizontal lines and three vertical lines, defining the dot pattern shown in Fig. 4, were chosen. Measuring the calibration points using total station was motivated by the fact that we had no access to the architectural plans of the building. On the other hand, there is no guarantee that the real elements of the building coincide with those in the plans. We had to determine the coordinates of the calibration points using angular measurements because the total station did not allow measuring distances exceeding 100 m. We applied the direct intersection method (Domínguez, 1993). Observations were made from two stations. One of them had arbitrary local coordinates, and provided those for the other station and for all calibration points. The coordinates of the second station were obtained with an error of 12 mm. In this process we used Leica Geo Office software to obtain the coordinates of all calibration points with a root mean square (RMS) error of 53 mm, eliminating the points with residuals exceeding this quantity. We did the camera calibration for three focal lengths (85, 95 and 130 mm). We used the coordinates of the calibration points to obtain the k_i coefficients in Eq. (1) and

the position of the PPS, and finally calibrated the focal length using 102 points (Table 1).

d. Image preparation

One of the problems of fieldwork in extreme environments is that they often do not allow the repetition of field observations. Consequently, it is extremely important to collect as much data as possible during the observations (in our case, taking a large number of photographs), so that errors which are detected back in the office can be corrected or, at least, minimized. To minimize errors, we did a selection of photographic peer models with an overlap of 80 %. We also corrected distortion of all photographs using internal orientation parameters and generated a new set of distortion-corrected images (Fig. 5), which can be used by any photogrammetric software.

e. Calculation of ground coordinates

Taking the radial distortion-free photographs as a starting point, we applied collinearity conditions using the known control points to obtain the parameters of different transformations (Helmert 3D transformations), with which the ground coordinates of any point on the photographs can be retrieved. We used a total of 10 photos to make 9 models, with estimated errors $\sigma_{xy} = 0.70$ m, $\sigma_z = 0.55$ m. Note that in this case the altimetry error is lower than the planimetry error because the X - Z plane is parallel to the glacier calving front (Fig. 2). Once all parameters are calculated from different transformations, the photographs are introduced, together with these parameters, into our in-house developed software that allows the photogrammetric restitution, without the need of artificial stereoscopic vision (Fig. 6), using semi-automatic correlation (Luhmann et al., 2006).

Johnsons Glacier front has two main lines requiring photogrammetric restitution. The upper one is the top of the cliff of the calving front and the lower one is the waterline on the calving front. The calving front, as usual, is heavily crevassed (Fig. 7b), which facilitates the use of automatic correlation. An orthophoto corresponding to a total of 180 000 points produced by automatic correlation is shown in Fig. 7a, and the restitution of the upper and lower lines of the glacier front, as well as the main crevasses and/or fractures, are shown in Fig. 7b.

2.4 Surface-based GNSS measurements of the land-terminating fronts of Hurd Glacier

In addition to the positions of the land-terminating fronts of Sally Rocks, Las Palmas and Argentina lobes of Hurd Glacier determined from aerial photos (BAS flight of 1957 and UKHO flight of 1990) or satellite images (Quickbird images of 2007 and 2010), researchers from GSNCI have

Table 1. Coefficients of radial distortion and position for PPS. The two last columns show the RMS error and the maximum error for radial distortion respectively. We considered 102 points for the polynomial adjustment. The first column shows the values for the calibrated focal lengths (mm).

Focal mm	Points	x_0	y_0	k_1	k_2	k_3	σ	σ_{\max}
85.23	102	1975 px	608 px	1.25213889313851E-08	-4.53330480188616E-15	4.48262617928856E-22	1 px	15 px
94.28	102	2043 px	602 px	1.18819659796645E-08	-4.07129365804265E-15	3.78566248003642E-22	1 px	13 px
131.50	102	2017 px	544 px	1.20656410994392E-08	-4.04403355146344E-15	3.68227991661486E-22	2 px	20 px



Figure 4. View of the facade of the building “Mirador”, where we did the calibration of the non-metric camera used for photographic shots of Johnsons Glacier front. In yellow, the points measured using a total station.

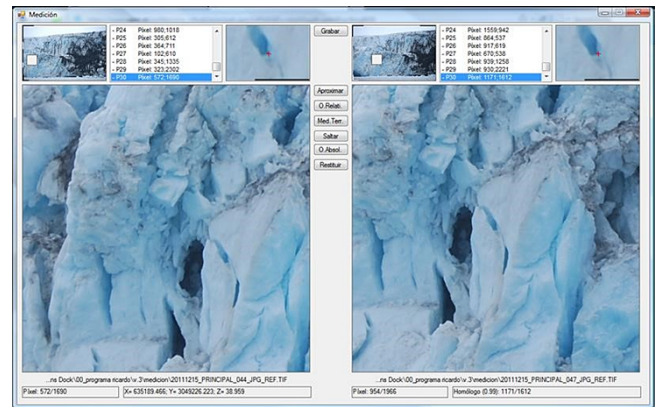


Figure 6. A snapshot of the main screen of our in-house developed software for photogrammetric restitution. This software does not require artificial stereoscopic vision for the restitution. By clicking on an item in the frame to the left, it locates the corresponding point in the right frame using automatic correlation.

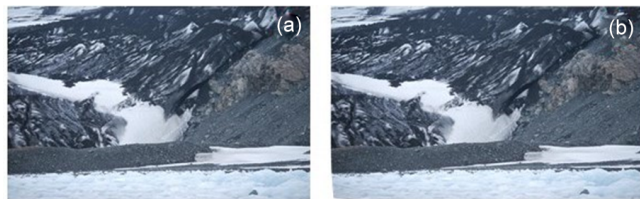


Figure 5. (a) Original image obtained with non-metric camera. (b) The rectified image, after applying the distortion function. At the lower left corner of the image an area affected by radial distortion can be seen.

measured the positions of these fronts several times during the period 2000–2012. The measurements were done using GNSS techniques (with a Trimble 5700 system, with Data Controller TSC2), with estimated horizontal accuracy between 0.07 and 0.60 m, depending on the campaign. The measurements were done either in real-time kinematics or in fast static (post-processed) mode. In all cases the GNSS base station was located at the neighboring Juan Carlos I station.

2.5 Processing of data from various sources and metadata compilation

Here we further discuss the compilation and processing of the data from the various sources, with an emphasis on those not discussed so far (aerial photos and satellite images), and we also summarize the errors for each one.

The first set of data (DOCU 1) corresponds to the British photogrammetric flight of 26 December 1957, performed at a flight altitude of 13 500 feet, using a metric camera IX Eagle Mk I and a nominal focal length of 153.19 mm. Once restored using Digi3D software, it allowed us to obtain the position of the different glacier fronts, including Johnsons Glacier (Table 2). The estimated horizontal accuracies range within 0.60–1.0 m. The earlier work by Molina et al. (2007) also used these same photographs for 3-D restitution, but, as mentioned in the Introduction, they used paper-printed photos (implying additional distortion) while we used digitized versions from the original films. Moreover, in the current study we use the images only to get the planimetry at sea level, so we reach a better accuracy. Using the certificate of calibration for IX Eagle Mk I, we have rectified the photos and then georeferenced the photograms X26FID0052160 and X26FID0052131 using ARCGIS software with an 8-parameter transformation.

Table 2. ARCGIS shape files for the BAS photogrammetric flight of 1957. In the third column the RMS error is shown.

Filename	Year	σ_{xy} (m)	Geomatic acquisition method
CNDP-ESP_SIMRAD_FRONT_JOHNSON_1957.shp	1957	± 0.60	Photogrammetric restitution, DOCU 1.
CNDP-ESP_SIMRAD_FRONT_SALLY_1957.shp	1957	± 1.20	Photogrammetric restitution, DOCU 1.
CNDP-ESP_SIMRAD_FRONT_LAS_PALMAS_1957.shp	1957	± 1.20	Photogrammetric restitution, DOCU 1.
CNDP-ESP_SIMRAD_FRONT_ARGENTINA_1957.shp	1957	± 1.20	Photogrammetric restitution, DOCU 1.

Table 3. ARCGIS shape files for the UKHO photogrammetric flight of 1990. In the third column the RMS error is shown.

Filename	Year	σ_{xy} (m)	Geomatic acquisition method
CNDP-ESP_SIMRAD_FRONT_JOHNSON_1990.shp	1990	± 2.00	Photogrammetric restitution, DOCU 2.
CNDP-ESP_SIMRAD_FRONT_SALLY_1990.shp	1990	± 2.00	Photogrammetric restitution, DOCU 2.
CNDP-ESP_SIMRAD_FRONT_LAS_PALMAS_1990.shp	1990	± 2.00	Photogrammetric restitution, DOCU 2.
CNDP-ESP_SIMRAD_FRONT_ARGENTINA_1990.shp	1990	± 2.00	Photogrammetric restitution, DOCU 2.

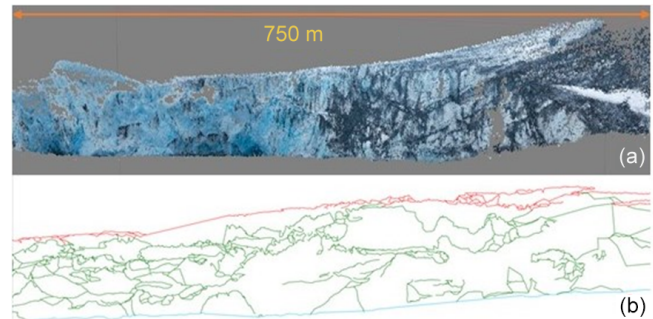
Table 4. ARCGIS shape file corresponding to the satellite image of QUICKBIRD system program (2010). The image is corrected to sea level to obtain the correct planimetric position of Johnsons Glacier calving front. In the third column the RMS error is shown.

Name	Year	σ_{xy} (m)	Geomatic acquisition method
CNDP-ESP_SIMRAD_FRONT_JOHNSON_2010.shp	2010	± 0.60	Aerial photo, DOCU 4.

The second set of data (DOCU 2) corresponds to another British photogrammetric flight, done in January 1990. In this case, a helicopter based on the ship HMS Endurance was used as platform, at a flight altitude of 10 000 feet, using a metric camera RMK A 15/23 with a nominal focal length of 153 mm. Once restored the data using the same Digi3D software as before, we obtained the position of the different glacier fronts, including Johnsons Glacier (Table 3). The estimated horizontal accuracy is 2.0 m.

DOCU 3 corresponds to the photogrammetric survey of Johnsons Glacier front made in 1999 by researchers from the University of Barcelona using a metric camera. However, this has not been considered in the current study because they only determined the top of the calving front cliff and not the position of the waterline, which is the line of interest to us (it is what we are comparing for the various images of Johnsons Glacier calving front).

DOCU 4 corresponds to an image captured in January 2010 by the Quickbird image system, which covers the entire work area. It is a raster file format GEOTIFF UTM 20S on the ellipsoid WGS84. Its original name was 10JAN29132854-P2AS052832138010_01_P001.TIF and it was obtained from <http://www.euspaceimaging.com> with reference ID 101001000B044C00. It is a black and white image with 16 bit digital values, but actually quantization levels are reduced to 11 bits. We restored this image using ARCGIS software to get a shape file with the position of Johnsons Glacier front (Table 4), upon rectification of the image to a horizontal plane at sea level using a projective transformation (Shan, 1999). The estimated horizontal accuracy is 0.60 m.

**Figure 7.** (a) Orthophoto of Johnsons Glacier calving front. This point cloud is made up of 180 000 points obtained by automatic correlation. (b) Johnsons Glacier calving front: in the upper part, in red, the uppermost line of the calving front, obtained by photogrammetric restitution; in the lower part, in blue, the waterline.

DOCU 5 is another Quickbird system image, taken in February 2007, which also covers the entire work area (with the exception of an insignificant rock outcrop to the north-west). It is a raster file format GEOTIFF UTM 20S on the ellipsoid WGS84. Its original name was 07FEB03135449-M2AS-052422572010_01_P001.TIF and it was obtained from <http://www.euspaceimaging.com>. It is an RGB color image with 16 bit digital values and an extra layer of near-infrared at 16 bits, but actually quantization levels are reduced to 11 bits. We restored this image using ARCGIS software to get a shape file with the positions of Johnsons Glacier and Las Palmas Glacier fronts (Table 5). This image was also

rectified to a horizontal plane at sea level, using a projective transformation. The estimated horizontal accuracy is 2.30 m.

DOCU 6 corresponds to the surface-based GNSS measurements of the land-terminating fronts of Hurd Glacier discussed in Sect. 2.3 (Blewitt et al., 1997). The data compilation, with their estimated accuracies (ranging between 0.07 and 0.60 m), is shown in Table 6.

Finally, DOCU 7 corresponds to the photogrammetric survey of Johnsons Glacier front done by the authors in February 2013 with a non-metric camera, discussed in Sect. 2.2. The corresponding metadata are given in Table 7. The estimated horizontal accuracy is 0.70 m.

3 Results and discussion: evolution of the glacier fronts during recent decades

3.1 Johnsons Glacier

The position of Johnsons Glacier calving front (the waterline position) at the beginning and end of 1957 is shown in Fig. 8, while its position for various years within the period 1957–2013 is shown in Fig. 9. As Johnsons is a tidewater glacier, its front position changes, though influenced by climate, are mostly driven by its internal dynamics, including feedback mechanisms involving the balance of forces, the flow and calving. We observe that the calving front advanced 74 m in its central part (segment A) between 1957 and 1990. Then the glacier front retreated 171 m (sum of the segments A, L and F) between 1990 and 2007, to remain stable until 2010 and then re-advance by 31 m in its central part (segment L) between 2010 and 2013. In spite of this latter re-advance of the central part, the southern part of the front retreated ca. 57 m (segment J) during the same period 2010–2013. Also note that, in the northern part, the glacier front has retreated over 97 m between 1957 and 2013 (E segment). The position of the front in the neighbourhood of segment E was estimated using the photo X26FID0093015 obtained at the beginning of 1957 (Rodríguez, 2014) from an incomplete BAS photogrammetric flight, shown in Fig. 8a.

The darker area seen on Fig. 8, in the southwestern area of the terminal part of the glacier, corresponds to an accumulation, due to intense folding and faulting in this part of Johnsons Glacier, of volcanic ash from tephra layers stemming from the volcanic eruptions at the neighboring Deception Island (Ximenis et al., 2000).

3.2 Sally Rocks front of Hurd Glacier

In this case, the front position changes are shown in Fig. 10. Hurd is a land-terminating glacier, which implies that the front position changes are mainly driven by climate-induced variations (e.g., increased melting), coupled with the (slow) dynamic response to the climate variations (due, e.g., to geometry changes associated to accumulation-ablation changes or variation in basal lubrication because of changes in the

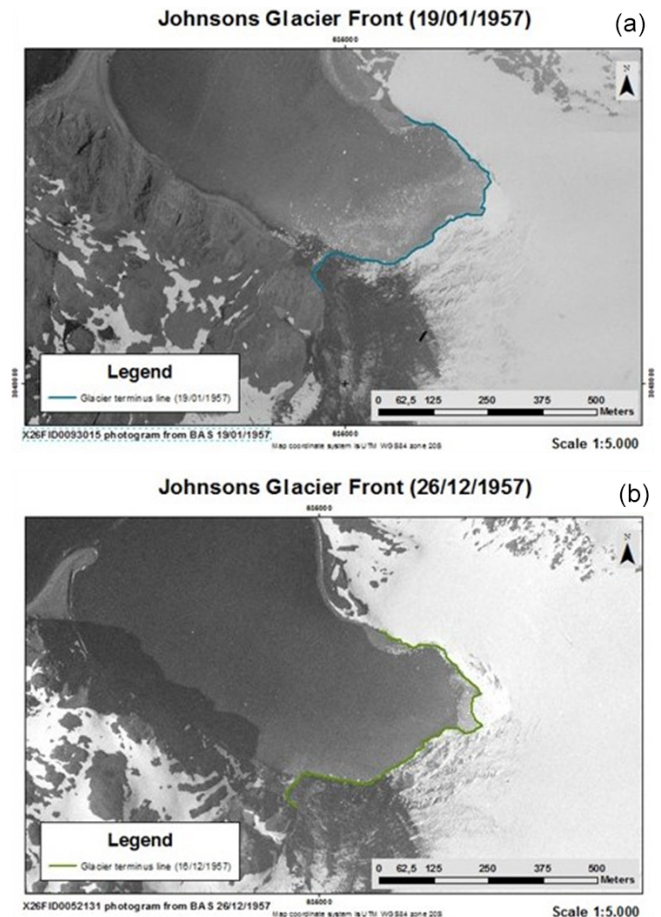


Figure 8. (a) Position of Johnsons Glacier calving front at the beginning of 1957 (blue line). The base map corresponds to the BAS photogrammetric flight of date 19 January 1957. This flight was not completed, and it can only be used for planimetric measurements at sea level. (b) Position of Johnsons Glacier calving front at the end of 1957 (green line). The base map corresponds to the BAS photogrammetric flight of date 26 December 1957. The scale of the figure does not match with the numerical map scale indicated.

amount of meltwater reaching the glacier bed). We observe that the glacier front retreated by 116 m in its central area (segment A) between 1957 and 1990. This was followed by a further retreat by 60 m (segment B) between 1990 and 2000, and yet further retreats by 47 m (C segment) during 2000–2006, and by 36 m (D segment) during 2006–2009. From 2009, the front position has remained stable until 2012. These changes are consistent with the overall warming trend in the South Shetland Islands, where the decade 1995–2006 has been the warmest since the 1960s, while the decade 2006–2015 has been colder than the previous one (by 0.5 °C in the summer and 1.0 °C in the winter; Oliva et al., 2016), and also with the mass balance record, which shows a shift to predominantly positive (i.e., mass gains) surface mass balances in Hurd and Johnsons glaciers starting around 2007/2008 (Navarro et al., 2013).

Table 5. ARCGIS shape file corresponding to the satellite image of QUICKBIRD system program (2007). The image is corrected to sea level to obtain the correct planimetric position of the glacier fronts. In the third column the RMS error is shown.

Name	Year	σ_{xy} (m)	Geomatic acquisition method
CNDP-ESP_SIMRAD_FRONT_JOHNSON_2007.shp	2007	± 2.30	Aerial photo, DOCU 5.
CNDP-ESP_SIMRAD_FRONT_LAS_PALMAS_2007.shp	2007	± 2.30	Aerial photo, DOCU 5.

Table 6. ARCGIS shape files corresponding to the GSNCI data inventory for Argentina, Las Palmas and Sally Rocks fronts of Hurd Glacier, determined using GNSS techniques. In the third column the RMS error is shown.

Name	Year	σ_{xy} (m)	Geomatic acquisition method
CNDP-ESP_SIMRAD_FRONT_SALLY_2000_2001.shp	2000	± 0.07	GNSS pole, DOCU 6.
CNDP-ESP_SIMRAD_FRONT_SALLY_2004_2005.shp	2005	± 0.60	GNSS backpack, DOCU 6.
CNDP-ESP_SIMRAD_FRONT_SALLY_2005_2006.shp	2006	± 0.60	GNSS backpack, DOCU 6.
CNDP-ESP_SIMRAD_FRONT_SALLY_2007_2008.shp	2008	± 0.07	GNSS pole, DOCU 6.
CNDP-ESP_SIMRAD_FRONT_SALLY_2008_2009.shp	2009	± 0.60	GNSS backpack, DOCU 6.
CNDP-ESP_SIMRAD_FRONT_SALLY_2009_2010.shp	2010	± 0.07	GNSS pole, DOCU 6.
CNDP-ESP_SIMRAD_FRONT_SALLY_2010_2011.shp	2011	± 0.07	GNSS pole, DOCU 6.
CNDP-ESP_SIMRAD_FRONT_SALLY_2011_2012.shp	2012	± 0.07	GNSS pole, DOCU 6.
CNDP-ESP_SIMRAD_FRONT_LAS_PALMAS_2000_2001.shp	2000	± 0.07	GNSS pole, DOCU 6.
CNDP-ESP_SIMRAD_FRONT_LAS_PALMAS_2004_2005.shp	2005	± 0.60	GNSS backpack, DOCU 6.
CNDP-ESP_SIMRAD_FRONT_LAS_PALMAS_2005_2006.shp	2006	± 0.60	GNSS backpack, DOCU 6.
CNDP-ESP_SIMRAD_FRONT_LAS_PALMAS_2007_2008.shp	2008	± 0.07	GNSS pole, DOCU 6.
CNDP-ESP_SIMRAD_FRONT_LAS_PALMAS_2008_2009.shp	2009	± 0.60	GNSS backpack, DOCU 6.
CNDP-ESP_SIMRAD_FRONT_LAS_PALMAS_2009_2010.shp	2010	± 0.07	GNSS pole, DOCU 6.
CNDP-ESP_SIMRAD_FRONT_LAS_PALMAS_2010_2011.shp	2011	± 0.07	GNSS pole, DOCU 6.
CNDP-ESP_SIMRAD_FRONT_LAS_PALMAS_2011_2012.shp	2012	± 0.07	GNSS pole, DOCU 6.
CNDP-ESP_SIMRAD_FRONT_ARGENTINA_2000_2001.shp	2000	± 0.07	GNSS pole, DOCU 6.
CNDP-ESP_SIMRAD_FRONT_ARGENTINA_2004_2005.shp	2005	± 0.60	GNSS backpack, DOCU 6.
CNDP-ESP_SIMRAD_FRONT_ARGENTINA_2005_2006.shp	2006	± 0.60	GNSS backpack, DOCU 6.
CNDP-ESP_SIMRAD_FRONT_ARGENTINA_2007_2008.shp	2008	± 0.07	GNSS pole, DOCU 6.
CNDP-ESP_SIMRAD_FRONT_ARGENTINA_2008_2009.shp	2009	± 0.60	GNSS backpack, DOCU 6.
CNDP-ESP_SIMRAD_FRONT_ARGENTINA_2009_2010.shp	2010	± 0.07	GNSS pole, DOCU 6.
CNDP-ESP_SIMRAD_FRONT_ARGENTINA_2010_2011.shp	2011	± 0.07	GNSS pole, DOCU 6.
CNDP-ESP_SIMRAD_FRONT_ARGENTINA_2011_2012.shp	2012	± 0.07	GNSS pole, DOCU 6.

The black spots on the glacier surface seen in Figure 10 are mostly ash from tephra layers, but these are often mixed with subglacial sediments taken to the glacier surface through fractures associated to thrust faults in the glacier snout resulting from the compressional regime. The compressional regime is mainly a consequence of fact that the glacier snout is frozen to bed (Molina et al., 2007; Navarro et al., 2009; Molina, 2014). This mixture of volcanic ash and subglacial sediments often accumulates at the surface in the form of pinnacles. According to Molina (2014, p. 126–127), most tephra shown in Fig. 10 likely correspond to eruptions well before 1829 (what is denoted as “oldest layers” in Ximenis et al., 2000, for Johnsons Glacier). We say likely because Molina did not analyze 1957 photos but images taken during 2004–2009, and did the geochemical analysis (X-ray fluorescence) with samples taken within this period. In any case, as Molina (2014) has pointed out, the tephra deposits in these terminal zones should not be used for purposes of dating

structures, because these spots in the terminal part of Hurd Glacier fronts are the result of accumulation of tephra flushed out, upon melting, from tephra layers corresponding to various eruptions. Consequently, the ash layers in this zone cannot be used to reliably infer past mass balance rates.

3.3 Las Palmas front of Hurd Glacier

The front position changes for Las Palmas Glacier are shown in Fig. 11. We can see that the glacier front retreated 11 m in its central part (segment A) between 1957 and 1990. Then, the front retreated 24 m (segment F) between 1990 and 2000. This was followed by a further retreat by 17 m (segment B) during 2000–2005, another 14 m (D segment) during 2005–2007, and finally another 10 m during 2007–2009, to remain stable thereafter. For Las Palmas front, the retreat during the period 1957–1990 was significantly lower than that for Sally Rocks front. This is likely due to the fact that, in 1957,

Table 7. ARCGIS shape file corresponding to the photogrammetric restitution of the Johnsons Glacier calving front in February 2013. The photo was obtained with a non-metric camera. In the third column the RMS error is shown.

Name	Year	σ_{xy} (m)	Geomatic acquisition method
CNDP-ESP_SIMRAD_FRONT_JOHNSON_2013.shp	2013	± 0.70	Photogrammetric restitution, DOCU 7.

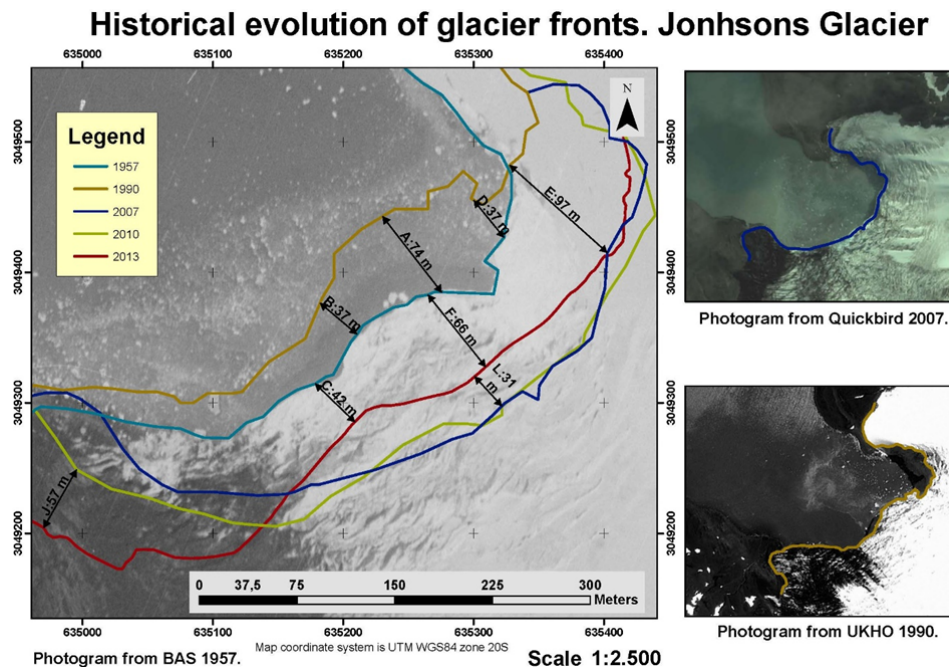


Figure 9. Calving front position changes of Johnsons Glacier. The oldest front position available corresponds to 1957 (in light blue) and the most recent to 2013 (in red). The base map corresponds to the BAS aerial photograph taken on 19 January 1957. The scale of the figure does not match with the numerical map scale indicated.

Las Palmas front ended at sea, and thus had a comparatively larger thickness at its terminal zone as compared with Sally Rocks front.

3.4 Argentina front of Hurd Glacier

In this case, shown in Fig. 12, the glacier front seems to have advanced by a small amount, ca. 5 m, in its central area (segment A) between 1957 and 1990. Then the front retreated by 70 m (segment A + segment B) between 1990 and 2000, to retreat another 15 m (C segment) during 2000–2005, a further 6 m during 2005–2008 (segment D) and yet another 14 m (segment I) until 2009, to remain stable since then. The apparent small advance between 1957 and 1990 does not fit with the overall retreating trend of the land-terminating fronts of Sally Rocks and Las Palmas. In fact, it could be due to a misinterpretation of the front position in 1990, due to remnants of snow cover on the terminal zone; or it could, instead, be real and have been induced by the dynamic response of this particular side lobe to climate changes, since each glacier reacts with different response times according

to its size and geometry (the observed change position is, in fact, very small).

4 Conclusions

The following conclusions may be drawn from our study:

1. Close-range photogrammetry with non-metric cameras is very suitable for determining the position of glacier fronts and, in particular, the calving fronts of tidewater glaciers, for which other techniques, such as surface-based GNSS measurements, are not possible. Moreover, it compares favorably in terms of costs with other methods such as photogrammetry with metric cameras or laser scanner systems. For the measurement of terminus position of land-terminating glaciers, surface-based GNSS techniques are fast and reliable. These surface-based techniques are effectively complemented, whenever available, with remote-sensing images, from either aerial photogrammetric flights or satellite optical imagery.

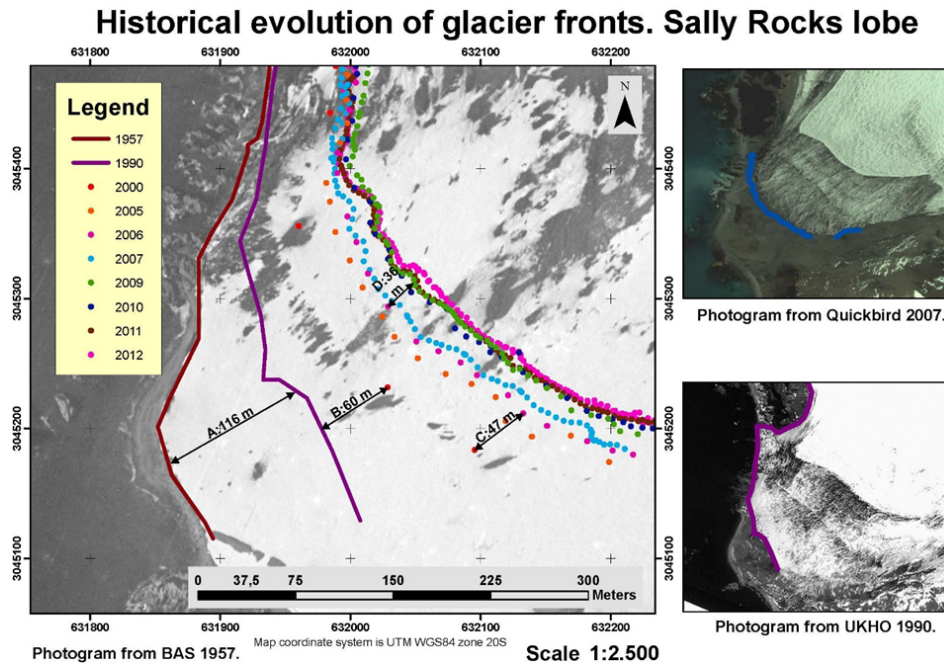


Figure 10. Terminus position changes of Sally Rocks front of Hurd Glacier. The oldest front position available corresponds to 1957 (in purple) and the latest to 2012 (in cyan). The base map corresponds to the BAS aerial photograph of 1957. The scale bar shown in the figure does not match with the map scale indicated.

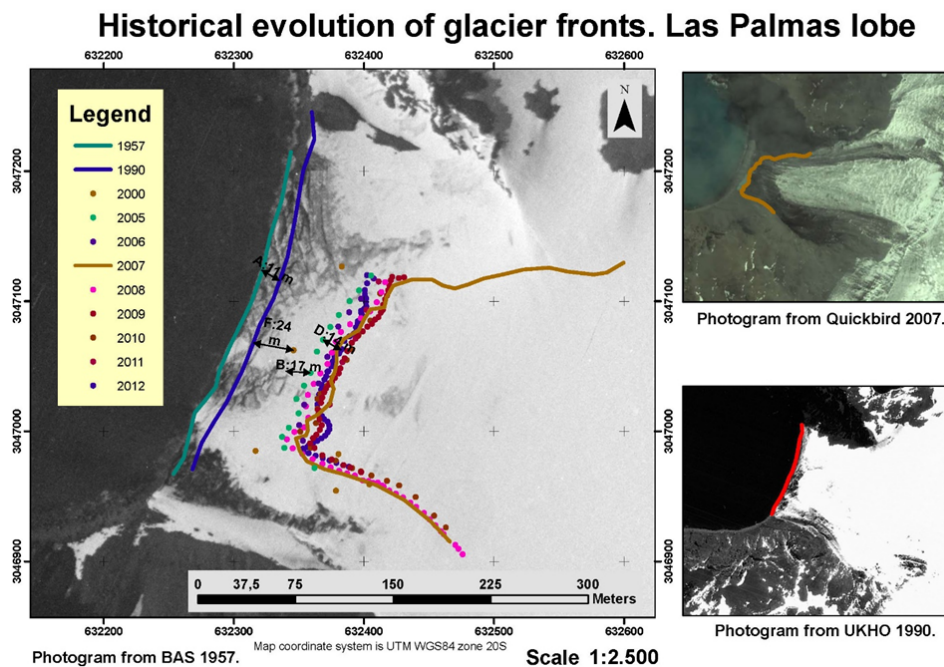


Figure 11. Terminus position changes of the front of Las Palmas side lobe of Hurd Glacier. The oldest front position available corresponds to 1957 (in green) and the latest to 2012 (blue points). The base map corresponds to the BAS aerial photograph of 1957. The scale bar shown in the figure does not match with the map scale indicated.

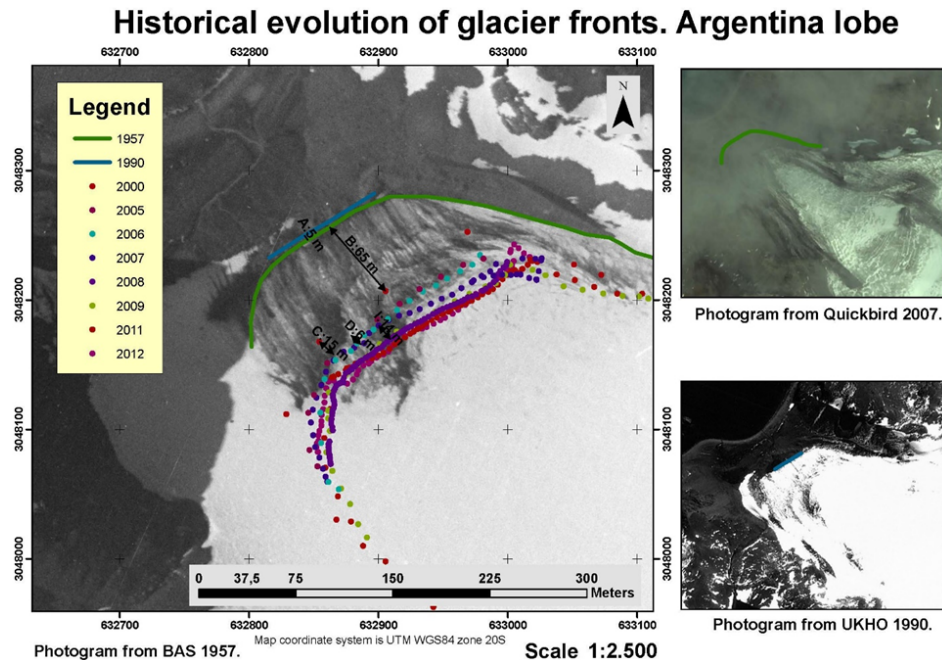


Figure 12. Terminus position changes of the front of Argentina side lobe of Hurd Glacier. The oldest front position available corresponds to 1957 (in purple) and the latest for the year 2012 (in cyan). The base map corresponds to the BAS aerial photograph of 1957. The outline marked on the “diffuse” 2007 Quickbird image corresponds to ground-based GNSS measurements. The scale bar shown in the figure does not match with the map scale indicated.

- The calving front of Johnsons Glacier has shown, during the period 1957–2013, several episodes of advance and retreat (and likely many more happened during long intermediate periods lacking observations). This is a tidewater glacier, so its front position changes, though can be influenced by climate, are mostly driven by the internal glacier dynamics, including various feedback mechanisms.
- The land-terminating fronts of Hurd Glacier (Sally Rocks, Las Palmas and Argentina) have experienced during the period 1957–2009 an overall retreating trend, remaining nearly stationary during 2009–2012. Being land-terminating, the front position changes are mostly driven by climate-related processes such as accumulation and melting variations, and their associated glacier dynamic response. The observed front variations are consistent with the regional climate changes. In particular, with an extremely warm 1995–2006 decade, followed by a colder 2006–2015 decade.

5 Data availability

<https://doi.pangaea.de/10.1594/PANGAEA.845379>
Study of the fronts of Johnsons and Hurd Glaciers (Livingston Island, Antarctica) from 1957 to 2013, with links to shapefiles.

Acknowledgements. This work was supported by grant CTM2014-56473-R from the Spanish National Plan of R&D.

Edited by: D. Carlson

Reviewed by: two anonymous referees

References

- ADD Consortium: Antarctic Digital Database, Version 3.0, database, manual and bibliography, Scientific Committee on Antarctic Research, Cambridge, 2000.
- Benjumea, B. and Teixidó, T.: Seismic reflection constrains on the glacial dynamics of Johnsons Glacier, Antarctica, *J. Appl. Geophys.*, 46, 31–44, 2001.
- Benjumea, B., Teixidó, T., Ximenis, L., and Furdada, G.: Prospección sísmica en el Glacier Johnsons, Isla Livingston (Antártida). (Campañas antárticas 1996–1997 y 1997–1998), *Acta Geológica Hispánica*, 34, 375–389, 1999.
- Benjumea, B., Macheret, Y. Y., Navarro F., and Teixidó, T.: Estimation of water content in a temperate glacier from radar and seismic sounding data, *Ann. Glaciol.*, 37, 317–324, 2003.
- Blewitt, G.: Basics of the GPS Technique: Observation Equations, Department of Geomatics, University of Newcastle, United Kingdom, 1997.
- Bliss, A., Hock, R., and Cogley, J. G.: A new inventory of mountain glaciers and ice caps for the Antarctic periphery, *Ann. Glaciol.*, 54, 191–199, 2013.
- Brown, D. C.: Close-range camera calibration, *PE&RS*, 37, 855–866, 1971.

- Calvet, J., García Sellés, D., and Corbera, J.: Fluctuaciones de la extensión del casquete glacial de la isla Livingston (Shetland del Sur) desde 1956 hasta 1996, *Acta Geológica Hispánica*, 34, 365–374, 1999.
- Domínguez, F.: *Topografía general y aplicada*, Ediciones Mundi-Prensa, Madrid, 1993.
- Directorate of Overseas Surveys (DOS): Sheet W62 58, British Antarctic Territory, South Shetland Island, Scale 1 : 200 000, 1968a.
- Directorate of Overseas Surveys (DOS): Sheet W62 60, British Antarctic Territory, South Shetland Island, Scale 1 : 200 000, 1968b.
- Furdáda, G., Pourchet, M., and Vilaplana, J. M.: Characterization of Johnsons Glacier (Livingston Island, Antarctica) by means of shallow ice cores and their tephra and ^{137}Cs contents. *Acta Geológica Hispánica*, 34, 391–401, 1999.
- Jonsell, U. Y., Navarro, F. J., Bañón, M., Lapazaran, J. J., and Otero, J.: Sensitivity of a distributed temperature–radiation index melt model based on AWS observations and surface energy balance fluxes, Hurd Peninsula glaciers, Livingston Island, Antarctica, *The Cryosphere*, 6, 539–552, doi:10.5194/tc-6-539-2012, 2012.
- Kraus, K.: *Photogrammetry, Vol. 1: Fundamentals and Standard Processes*, Dümmlers, 1993.
- Kraus, K.: *Photogrammetry. Geometry from Images and Laser Scans*, 2nd Edn., de Gruyter, 2007.
- Luhmann, T., Robson, S., Kyle, S., and Harley, I.: *Close Range Photogrammetry: Principles, Techniques and Applications*, Whittles Publishing, 2006.
- Macheret, Y. Y., Otero, J., Navarro, F. J., Vasilenko, E. V., Corcuera, M. I., Cuadrado, M. L., and Glazovsky, A. F.: Ice thickness, internal structure and subglacial topography of Bowles Plateau ice cap and the main ice divides of Livingston Island, Antarctica, by ground-based radio-echo sounding, *Ann. Glaciol.*, 50, 49–56, 2009.
- Martín, C., Navarro, F. J., Otero, J., Cuadrado, M. L., and Corcuera, M. I.: Three-dimensional modelling of the dynamics of Johnsons glacier (Livingston Island, Antarctica), *Ann. Glaciol.*, 39, 1–8, 2004.
- Molina, C.: *Caracterización dinámica del glaciar Hurd combinando observaciones de campo y simulaciones numérica*, PhD Thesis, Universidad Politécnica de Madrid, 2014.
- Molina, C., Navarro, F., Calvet, J., García-Selles, D., and Lapazaran, J.: Hurd Peninsula glaciers, Livingston Island, Antarctica, as indicators of regional warming: ice-volume changes during period 1956–2000, *Ann. Glaciol.*, 46, 43–49, 2007.
- Navarro, F. J., Macheret, Y. Y., and Benjumea, B.: Application of radar and seismic methods for the investigation of temperate glaciers, *J. Appl. Geophys.*, 57, 193–211, 2005.
- Navarro, F. J., Otero, J., Macheret, Y. Y., Vasilenko, E. V., Lapazaran, J. J., Ahlstrøm, A. P., and Machío, F.: Radioglaciological studies on Hurd Peninsula glaciers, Livingston Island, Antarctica, *Ann. Glaciol.*, 50, 17–24, 2009.
- Navarro, F., Jonsell, U., Corcuera, M., and Martín-Español, A.: Decelerated mass loss of Hurd and Johnsons glaciers, Livingston Island, Antarctic Peninsula, *J. Glaciol.*, 59, 115–128, 2013.
- Oliva, M., Navarro, F., Hrbáček, F., Hernández, A., Nývlt, D., Pereira, P., Ruiz-Fernández, J., and Trigo, R.: Recent regional cooling of the Antarctic Peninsula and its impacts on the cryosphere, *Nature Communications*, submitted, 2016.
- Osmanoglu, B., Navarro, F. J., Hock, R., Braun, M., and Corcuera, M. I.: Surface velocity and mass balance of Livingston Island ice cap, Antarctica, *The Cryosphere*, 8, 1807–1823, doi:10.5194/tc-8-1807-2014, 2014.
- Otero, J., Navarro, F. J., Martín, C., Cuadrado M. L., and Corcuera, M. I.: A three-dimensional calving model: numerical experiments on Johnsons Glacier, Livingston Island, Antarctica, *J. Glaciol.*, 56, 200–214, 2010.
- Palà, V., Calvet, J., García-Sellés, D., and Ximenis, L.: Fotogrametría terrestre en el Glaciar Johnsons, Isla Livingston, Antártida, *Acta Geológica Hispánica*, 34, 427–445, 1999.
- Pfeffer, T., Arendt, A., Bliss, A., Bolch, T., Cogley, J. G., Gardner, A. S., Hagen, J. O., Hock, R., Kaser, G., Kienholz, C., Miles, E. S., Moholdt, G., Moelg, N., Paul, F., Radić, V., Rastner, P., Raup, B. H., Rich, J., Sharp, M. J., and the Randolph Consortium: The Randolph Glacier Inventory: a globally complete inventory of glaciers, *J. Glaciol.*, 60, 537–552, 2014.
- Rodríguez, R.: *Integración de modelos numéricos de glaciares y procesado de datos de georradar en un sistema de información geográfica*, PhD Thesis, Universidad Politécnica de Madrid, 2014.
- Rodríguez, R. and Navarro, F.: Study of the fronts of Johnsons and Hurd Glaciers (Livingston Island, Antarctica) from 1957 to 2013, Universidad Politécnica de Madrid, <https://doi.pangaea.de/10.1594/PANGAEA.845379>, 2015.
- Shan, J. J.: *A Photogrammetric Solution for Projective Reconstruction*, Department of Geomatics Engineering, Purdue University, SPIE Conference on Vision Geometry VIII, Denver, Colorado, 296–304, 1999.
- Wolf, P. R.: *Elements of Photogrammetry with Air Photo Interpretation and Remote Sensing*, Second Edition, McGraw-Hill Book Company, New York, 1983.
- Ximenis, L.: *Dinàmica de la Glacera Johnsons (Livingston, Shetland del Sud, Antártida)*, PhD Thesis, University of Barcelona, 2001.
- Ximenis, L., Calvet, J., Enrique, J., Corbera, J., Fernández de Gamboa C., and Furdáda, G.: The measurement of ice velocity, mass balance and thinning-rate on Johnsons Glacier, Livingston Island, South Shetland Islands, Antarctica, *Acta Geológica Hispánica*, 34, 403–409, 1999.
- Ximenis, L., Calvet, J., García, D., Casas, J. M., and Sàbat, F.: Folding in the Johnsons glacier, Livingston Island, Antarctica, in: *Deformation of Glacial Materials*, edited by: Maltman, A. J., Hubbard, B. A., and Hambrey, M. J., The Geological Society London, special publ., 176, 147–157, 2000.